

Crystallization and physicochemical investigation of melevodopa hydrochloride, a commercially available antiparkinsonian active substance

TAMÁS KISS, GÁBOR KATONA, RITA AMBRUS*

*Institute of Pharmaceutical Technology and Regulatory Affairs, University of Szeged,
Eötvös Street 6, 6720 Szeged, Hungary*

*Corresponding author: Rita Ambrus

E-mail: ambrus.rita@szte.hu

Received: 11 May 2021 / Revised: 22 June 2021 / Accepted: 23 June 2021

Abstract: In this work, the levodopa methyl ester was crystallized from different solvents and its physicochemical properties were explored. This active pharmaceutical ingredient (API) is commercially available as an effervescent tablet in Italy. The crystallization methods were solvent evaporation from different solvents (water, ethanol, methanol) and crystallization by adding an antisolvent. These methods led to the same product which had the same different X-ray powder diffractogram that was different from the diffractogram of LDME-I. According to the hot-stage microscopy and differential scanning calorimetry (DSC), the melting point was remarkably decreased, however, above the melting point, the melt tended to recrystallize to the LDME-I which was shown by an exothermic peak on the DSC curve. This was verified by an additional test during which the API was heated to 145 °C, thereafter the diffractogram matched perfectly with the LDME-I. These results indicate the presumable formation of a new polymorph. During the crystallization, the LDME did not degrade according to the high-performance liquid chromatography. Besides the recrystallization kinetics of the amorphous form was also followed, the activation energy of recrystallization was 85.3 kJ/mol, the diffractogram of recrystallization was the same as in the case of the crystallized products.

Keywords: *melevodopa hydrochloride, crystallization, potential polymorph, melting point, X-ray powder diffractometry*

1. Introduction

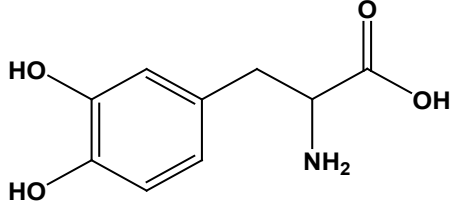
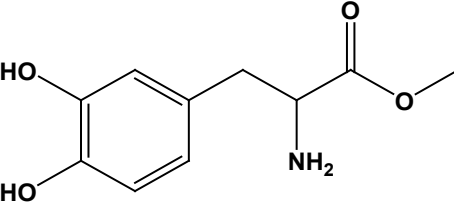
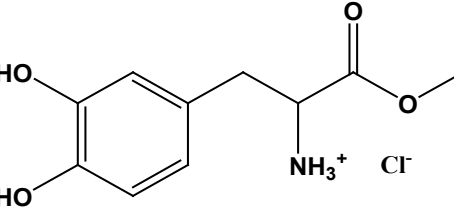
Levodopa (LD) is the most widely applied active pharmaceutical agent (API) in the treatment of Parkinson's disease, however, it suffers from some disadvantages, like levodopa-related motor complications (LRMCs). Approximately 50% to 80% of patients with Parkinson's disease experience LRMCs after 5 to 10 years of LD treatment (1).

The solubility of LD is limited: 5.0 mg/mL in water (2), therefore intensive research was conducted to find highly soluble LD derivatives as an alternative (3). Among the LD alternatives, the most promising candidate was the levodopa methyl ester hydrochloride (melevodopa hydrochloride, LDME). This API has about 250-fold higher water solubility than the LD, therefore high doses can be prepared in liquid formulations (4) and its absorption ability is higher due to the higher lipophilicity (Table 1). Both of LD and LDME have a tendency to decompose in a pH-dependent pathway. The advantage of LDME is that its main degradation product is LD (5), which still has an antiparkinsonian effect, in contrast to the degradation products of LD (6).

The LDME is marketed as an effervescent tablet in Italy (brand name: Sirio[®], manufacturer: Chiesi Farmaceutici SpA, Parma, Italy). The doses are 314 mg of LDME/25 mg of carbidopa; 157 mg of LDME/12.5 mg of carbidopa; 125.6 mg of LDME/25 mg of carbidopa (10,11). Based on the molecular mass ratio, 1.256 mg LDME is equivalent to 1.000 mg of LD (12). The advantage of the effervescent tablets is that the liquid formulations can pass more easily through the stomach, therefore the erratic gastric emptying effect is lower causing quicker onset. According to the Cambridge Crystallographic Data Centre (CCDC) (13), only one X-ray diffractogram is assigned to the LDME.

The main purpose of ICH guidelines is to provide patient safety. One of the remarkable risks is the change in the dissolution profile that can occur as a result of e. g. a polymorphic change. The ICH Q6A guideline defines polymorphism as „some drug substances exist in different crystalline forms which differ in their physical properties. Polymorphism may also include solvation or hydration products (also known as solvatomorphism) and amorphous forms”. Only the imagination limits the possibilities of polymorph screening, among

Table 1 Chemical structure and molecular mass of the levodopa, melevodopa and its hydrochloride salt

| API | Chemical structure | Molecular weight (g/mol) | log P _{octanol/water} |
|--------------------------|---|--------------------------|--------------------------------|
| levodopa |  | 197.19 | -2.9 (7) |
| melevodopa |  | 211.21 | -0.21 (8) |
| melevodopa hydrochloride |  | 247.06 | 0.64 (9) |

which the crystallization by evaporation/cooling from a proper solvent/solvent mixtures (14), crystallization from supercritical fluid (15), exposure to vapour at high or low relative humidity (16), solid-state polymorphic transformation (17) and seeding/pseudoseeding (18). The polymorphs can modify the stability, solubility, and manufacturing properties. A drawback of LDME is the chemical instability (5), sensitivity to the temperature, and aqueous media, thus it has to be taken into consideration when carrying out the crystallization process.

In this study, we aimed to crystallize the LDME from different solvents and investigate the physical properties of products. Besides our purpose was also to follow the recrystallization from the amorphous state.

2. Materials and methods

2.1. Materials

The LDME (3,4-dihydroxyphenylalanine methyl ester hydrochloride), ethyl acetate and ethanol absolute (EtOH) were purchased from Merck (Budapest, Hungary). The methanol (MeOH) was obtained from VWR International Ltd (Debrecen Hungary).

2.2. The crystallization of LDME

20 mg of LDME was dissolved in 5 mL of EtOH, MeOH and water, the solubility also determined in these solvents. LDME was dissolved in different organic solvents and water. A Rotavapor R-125 equipment (BÜCHI Labortechnik AG, Flawil, Switzerland) was used to evaporate the solvent at decreased pressure and increased temperature. The rotation speed of the round-bottom flask was 135 rpm. The LDME products were LDME-EtOH, LDME-MeOH and LDME-water whose summarized name was "LDME-II" in this article, respectively which were compared to the starting material named as "LDME-I".

After the elimination of organic solvent some fraction of products was stored in a refrigerator (4±2 °C), another fraction was stored at 32±2 °C, 60±5 % relative humidity (RH) for one day. The recrystallized powders were investigated the next day to let the partially amorphous fraction recrystallize.

Besides previous experiments, LDME was also crystallized from 0.7 ml of EtOH (60 mg/mL) by adding ethyl acetate dropwise (0.1 mL/s) as an antisolvent to the solution in a beaker under constant 200 rpm stirring using a magnetic stirrer. During the procedure the solution became opal-

escent after adding 16 ml ethyl acetate. Further 14 mL of ethyl acetate was dropped to the solution to achieve a higher extent of crystallization. The resulting suspension was filtered by Whatman™ membrane (GE Healthcare Sciences, Chalfont St Giles, United Kingdom) and the residue was gently dried at 50 °C in a vacuum dryer (Binder GmbH, Tuttlingen, Germany).

The solubility of LDME was determined in water, MeOH and EtOH with a spectrophotometric method. This was carried out using UV-Vis spectrophotometry (ABL&E-Jasco UV/Vis Spectrophotometer V-740, Budapest, Hungary). The quantification wavelength was 280 nm, the calibration was done in 0.01-0.1 mg/mL concentration range in each solvent. After sampling from the supernatant, the saturated solution was diluted to obtain a solution in the range of calibration.

2.3. X-ray powder diffractometry (XRPD)

The samples crystallized from different organic solvents and water were investigated by a Bruker D8 Advance diffractometer (Bruker AXS GmbH, Karlsruhe, Germany). The powders were irradiated by Cu K_{α1} (λ=1.5406 Å), the intensity of X-rays were quantified by a VANTEC-1 detector. The samples were investigated at 40 kV voltage and 40 mA current in the range of 3°-40° 2θ at a step of 0.007°/0.1 sec. The samples were placed onto a quartz sample holder, then the samples were measured meanwhile the sample holder rotated.

All manipulations, including K_{α2}-stripping, background removal, and signal-to-noise smoothing of the area under the peaks of diffractograms were performed with DIFFRACTPLUS EVA software. The results were compared to the available data in the CCDC database.

2.4. The measurement and evaluation of recrystallization kinetics

The recrystallization kinetics of LDME from an amorphous state was also investigated with the help of a hot-humidity stage chamber conducted to XRPD (HH-XRPD), whereby temperature was variable. The API was dissolved in 0.5 mL of MeOH directly in the sample holder. The solvent was intensively evaporated in a vacuum dryer (Binder GmbH, Tuttlingen, Germany) at 50 °C, 100 mbar. Thereafter the solvent was removed, the residual amorphous, transparent LDME was placed in the instrument. An ANS-Sycoshot humidity control

device was connected to the XRPD, which injected humidity into a controlled dry gas flow. The carrier gas was compressed air with a 0.5 L/min flow. The sample was placed onto a Ni-coated sample holder. The RH was set at 40 °C, 60 °C, and 70 °C constant temperatures.

As a part of preformulation studies, HH-XRPD can provide information about polymorphic transformations and recrystallization kinetics, and short-term stability can be monitored *in situ*.

In this work, the recrystallization process of amorphous LDME was followed to determine the product and the kinetics of the process.

The parameters of recrystallization kinetics were modeled by the Avrami equation (19):

$$1 - \alpha = e^{-kt}, \quad (1)$$

where the α is the crystalline fraction of LDME, k is the rate constant, n is the Avrami index describing the characteristic of nucleation and crystal growth.

The Avrami parameters (K , n) can be determined from the equation (1) by transforming into a double logarithmic form:

$$\ln[-\ln(1 - \alpha)] = \ln k + n \ln t \quad (2)$$

If the $\ln [-\ln(1-\alpha)]$ is plotted as a function of $\ln t$, the slope will be equal to n , the intercept will be equal to $\ln k$.

The activation energy of recrystallization was also calculated by utilizing the temperature dependence of the Arrhenius equation (assuming that the recrystallization has first order kinetics):

$$\ln k = \ln A - \frac{E_a}{RT} \quad (3)$$

where k is the rate constant, A is the frequency factor, E_a is the activation energy, R is the gas constant and the T is temperature. Thus, based on the time dependence of the rate constant, the activation energy can be calculated.

2.5. Differential scanning calorimetry (DSC)

DSC measurements were carried out by a Mettler-Toledo 821e DSC instrument (Mettler-Toledo GmbH, Switzerland) under constant argon flow of 150 mL/min in the temperature range of 25-300 °C with a heating rate of 10 °C/min. The 3-5 mg of LDME was measured in crimped aluminium pans with three holes on the top. Data analysis was per-

formed using STARe software (Mettler-Toledo GmbH, Greifensee, Switzerland). Each result was normalized to sample size.

2.6. Thermogravimetric analysis (TGA)

The Mettler Toledo TGA 1 thermal analysis system (Mettler-Toledo GmbH, Greifensee, Switzerland) was applied to characterize the thermal stability of the LDME. 3-5 mg of the samples were placed in aluminium pans and measured in the temperature range of 25-300 °C with a heating rate of 10 °C/min under constant nitrogen flow of 50 mL/min. Data analysis was performed using STARe software (Mettler-Toledo GmbH, Greifensee, Switzerland). The results were normalized to the sample size.

2.7. Hot-stage microscopy (HSM)

The melting was also observed by hot-stage microscopy (HSM) using a LEICA Thermo microscope (LEICA MZ 6, Germany). The samples were placed under the microscope between two glass slides. 10 °C/min heating rate was applied for the measurements. Images were taken at 4-fold magnification. It helped to assign the peaks on the DSC and TGA curves. This simple investigation method was mainly useful when the peaks overlapped.

2.8. Scanning electron microscope (SEM) measurements

The morphological appearance of the different forms of LDME was checked with the help of scanning electron microscopy (SEM, Hitachi S4700, Hitachi Scientific Ltd., Tokyo, Japan) at 10 kV. All samples were coated with gold-palladium (90 s) by a sputter coater (Bio-Rad SC 502, VG Microtech, Uckfield, UK).

2.9. High-performance liquid chromatography (HPLC)

The LDME and the accidental degradation products were analysed by an Agilent 1260 HPLC system (Agilent Technologies, San Diego, United States). The mobile phase was composed of acetate buffer (0.022 M, pH=5.0):MeOH=90:10 (v/v). A Chrome-Clone™ 5 µm C-18 100 Å column (150 x 4.6 mm, Phenomenex, Torrance, CA, USA) was connected to a C-18 security guard cartridge. 10 µL of sample was injected and separation was

carried out with isocratic flow with 1 mL/min flow for 8 min at 30 °C. Before the HPLC measurement, the LDME was dissolved in MeOH. The LDME was analysed at 280 nm with a diode array detector. Data were evaluated with the help of ChemStation B.04.03. Software (Agilent Technologies, Santa Clara, United States). The calibration equation of LDME dissolved in MeOH under the circumstances of separation using the area under curve values:

$$y = 3392.4 x + 8.961 \quad (4)$$

where the unit of y is mAu*min, the unit of x is mg/mL, R^2 was 0.9985. The limit of detection (LOD) was 43.7 µg/mL and the limit of quantification (LOQ) was 144 µg/mL.

3. Results and discussion

3.1. The results of LDME crystallization

The solubility of the API in different solvents was determined. As a general phenomenon, the solubility was decreased when the polarity of the solvent was also decreased suggesting that the LDME prefers the polar media.

The exact process parameters of the evaporations are detailed in Table 2.

Table 2 The circumstances of solvent evaporation method and the solubility of LDME in the utilized solvents

| Solvent | T (°C) | p (mbar) | S _{LDME-I} (mg/mL) at 25 °C | S _{LDME-II} (mg/mL) at 25 °C |
|---------|--------|----------|--------------------------------------|---------------------------------------|
| EtOH | 65 | 200 | 105 | 31.8 |
| MeOH | 37 | 200 | 232 | 303 |
| Water | 90 | 50 | 912 | 614 |

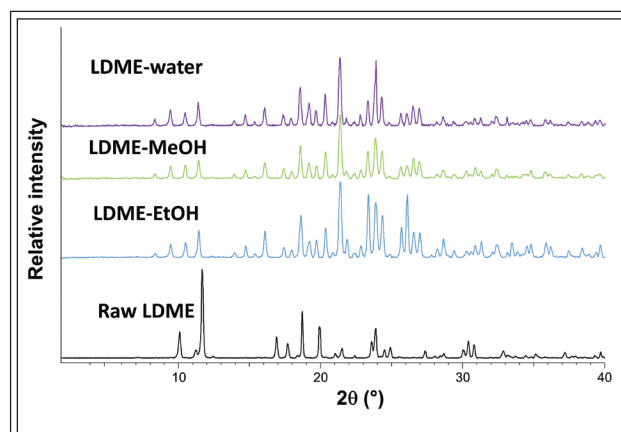


Figure 1 The XRP diffractogram of LDME-I and LDME-II

After dissolving the LDME in proper solvents and the crystallization led to products (LDME-water, LDME-MeOH, LDME-EtOH) which had the same XRP diffractogram (Figure 1) that could not be found nor in the literature, neither in the CCDC database. It was different from the diffractogram of the starting material (LDME-I). The starting material matched with the diffractogram of LDME in the CCDC. The solubility of two crystal forms differed, the LDME-I had higher solubility in water and EtOH, the LDME-II had a higher solubility in MeOH, however the solubility of both forms increased as the polarity of the solvent increased.

This result is in line with the statement in the literature that claims LDME is approximately 250-fold more soluble than LD in aqueous media (20).

The same diffractogram belonged to all crystallized products, however, the diffractogram of LDME-I was different. The characteristic peaks of the different forms of LDME are listed in the Table 3. Besides these results, the recrystallization process and the crystallization from EtOH with ethyl acetate antisolvent led to the same products. The obtained product did not seem to be a solvatomorph because the XRP diffractogram of the API was the same after crystallization from different solvents, it appeared to be a different crystalline form.

The chemical stability of LDME is low, therefore we had to make sure that the change on the diffractogram did not happen due to the chemical degradation. The change in the XRP diffractogram was not the result of chemical degradation based

on the HPLC investigations. According to the comparison of the chromatogram of the LDME-I and the products, there was no sign of degradation product after crystallization. The stability of the API in the used solvent (MeOH) was satisfactory for the measurements according to pre-experiments (no degradation product could be detected in 1-day storage at room temperature).

Table 3 Characteristic peaks of LDME-I and LDME-II on the diffractogram

| LDME-I | LDME-EtOH | LDME-MeOH | LDME-water |
|----------|-----------|-----------|------------|
| 11.027 ° | 9.364 ° | 9.349 ° | 9.335 ° |
| 12.145 ° | 10.419 ° | 10.408 ° | 10.415 ° |
| 12.566 ° | 11.430 ° | 11.405 ° | 11.419 ° |
| 17.625 ° | 12.333 ° | 12.312 ° | 12.314 ° |
| 19.370 ° | 16.834 ° | 16.815 ° | 16.844 ° |
| 20.560 ° | 19.284 ° | 19.249 ° | 19.265 ° |
| 24.095 ° | 21.965 ° | 21.958 ° | 21.969 ° |
| 24.368 ° | 23.881 ° | 23.842 ° | 23.869 ° |
| 29.018 ° | 24.375 ° | 24.372 ° | 24.425 ° |
| 30.690 ° | 24.838 ° | 24.816 ° | 24.805 ° |
| 33.067 ° | 26.524 ° | 26.507 ° | 26.530 ° |
| 37.269 ° | 35.974 ° | 35.894 ° | 35.955 ° |

3.2. The melting of the products

Usually, different melting point belongs to different polymorphs, therefore the DSC and HSM were additional measurements to verify the change in the crystalline state. Figure 2 shows the melting of the LDME based on the HSM investi-

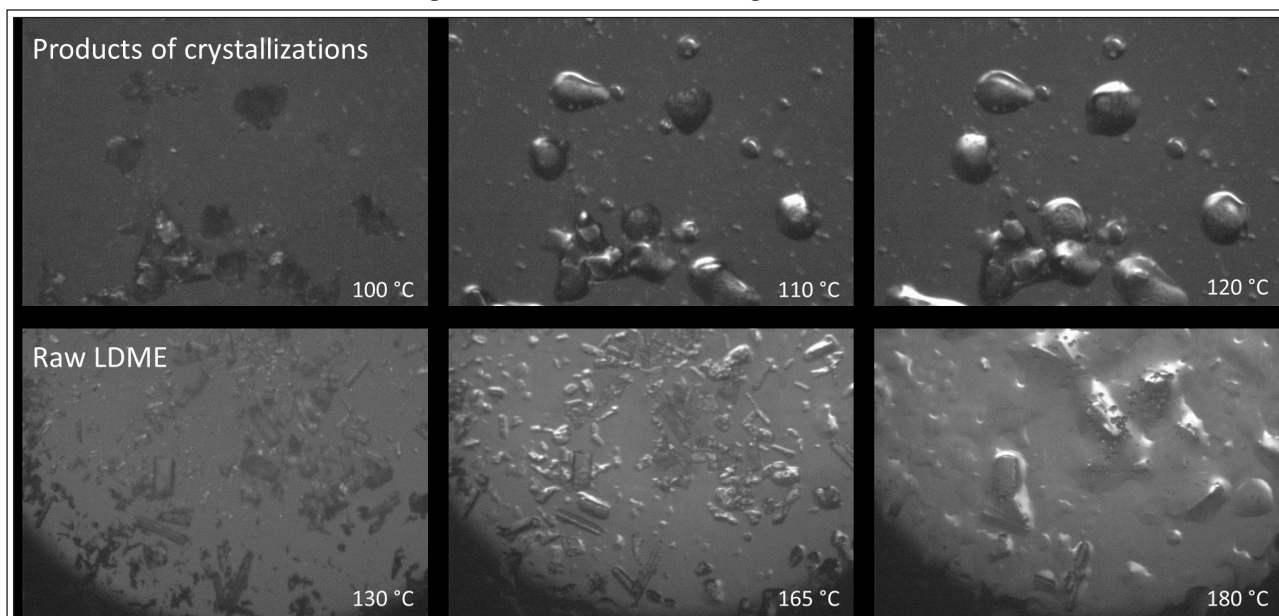
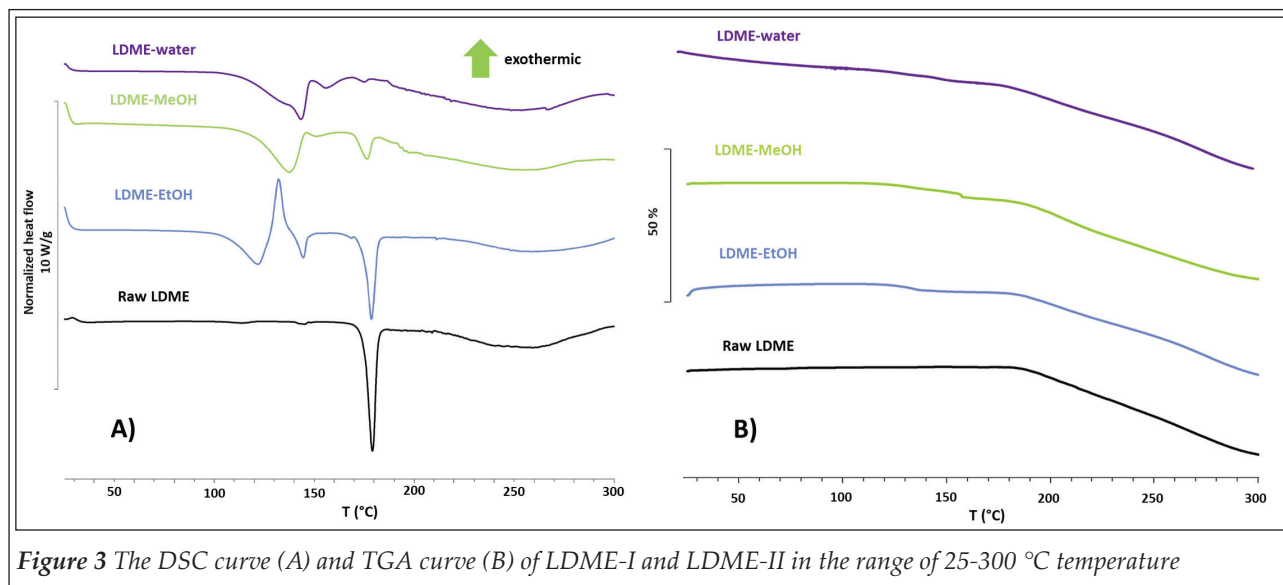


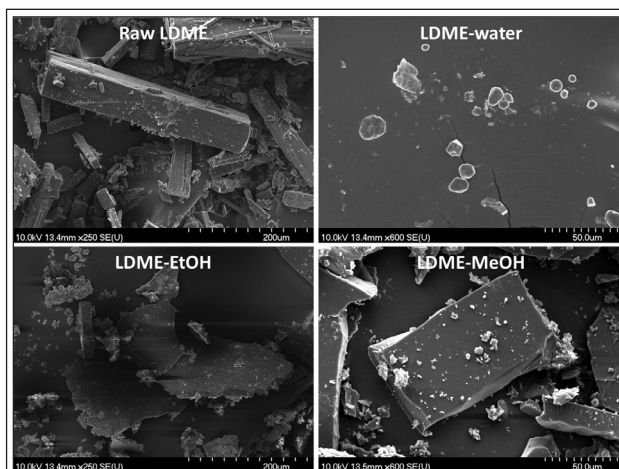
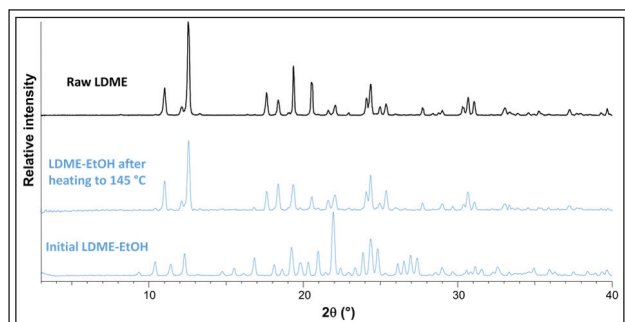
Figure 2 The results of HSM measurements, the top line represents the melting of LDME-I, the bottom line represents the melting of LDME-II (4x magnification)



gations. This measurement showed a remarkable decrease of the LDME melting point that was further investigated by DSC and TGA measurements.

The melting point of the products was remarkably decreased from 178 °C to approximately 138 °C as a result of the presumable polymorphic transformation (Figure 3/A). The exact determination of melting point was done after a single derivation of the DSC curve, after that, a local minimum on the derivative curve appeared at 138 °C belonging to the melting of the API. The LDME-MeOH had the same melting point, in this case, the local minimum of the original DSC curve was at 137 °C assigned to the melting of the LDME, as well. In the crystallized products, more peaks overlapped, HSM investigations verified that the melting begins at around 110 °C, in contrast to the melting point of LDME-I. The DSC curve of LDME-EtOH contained an intensive exothermic peak in the range of melting which peak also appears in the case of LDME-MeOH, however, its

intensity is lower. At the same time, the exothermic peak – which was the most intensive in the case of LDME-EtOH, moderately intensive in the case LDME-MeOH and its presence was not obvious in case of LDME-water – needed to be interpreted, therefore the LDME-EtOH was heated above this (to 145 °C). As an effect of heating, the diffractogram of LDME-EtOH matched the diffractogram of LDME-I (Figure 4). Thus, this exothermic peak could be assigned to the recrystallization of crystallized LDME to LDME-I. The intensity of the recrystallization peak on the DSC curve was in line with the appearance of the melting point of LDME-I at 178 °C. According to the TGA curve, the degradation temperature of the LDME was also decreased simultaneously with the melting point (Figure 3/B). Above this temper-



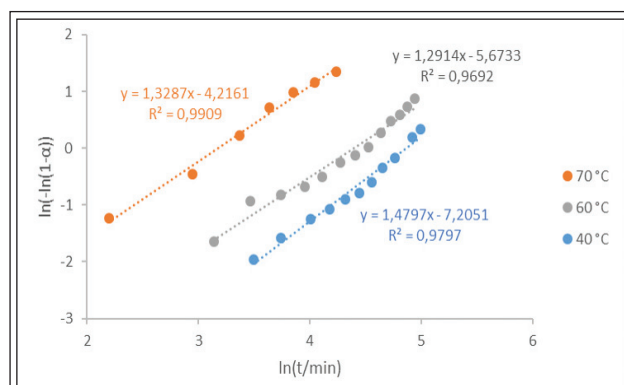


Figure 6 The evaluation of recrystallization kinetics of amorphous LDME to LDME-II

ature, the degradation slowed down, and in the case of all products of crystallization, this was due to the recrystallization to LDME-I, above the melting point of LDME-I, these products began degrading to a higher extent. These results also showed verification for the formation of the new presumable polymorph as a result of crystallization.

3.3. The morphology of the LDME forms

The LDME-I consisted of micro-sized, clearly cylindrically shaped particles. The shape of the particles depended on the treatment after solvent evaporation, their fracture was highly dependent on the method of removal from round-bottom flask or beaker, therefore the product of antisolvent method was proper to characterize the shape of the LDME-II crystals. The LDME-II particles was rather strawberry-like, consisted of more spherical compared to LDME-I (Figure 5).

3.4. Recrystallization kinetics of LDME

The amorphous LDME was immediately placed onto the sample holder after amorphization and the recrystallization kinetics was followed. The area of the whole diffractogram was summed up. Interestingly at all investigated temperatures, the characteristic peaks of LDME-II appeared on the diffractograms and instead of the peaks of LDME-I.

Applying the Avrami equation, the $\ln(-\ln(1-\alpha))$ was plotted as a function of $\ln t$ (Figure 6), the intercept was equal to $\ln k$.

The rate constants of recrystallization were calculated from the linear fit (Table 4).

Table 4 The rate constant of recrystallization from amorphous LDME to LDME-II at different temperatures

| T (°C) | k (1/min) |
|--------|-----------------------|
| 40 | 7.43×10^{-4} |
| 60 | 3.44×10^{-3} |
| 70 | 1.48×10^{-2} |

As a consequence of the Arrhenius equation, the temperature dependence of $\ln k$ values determined the activation energy of recrystallization from the amorphous state. The E_a of recrystallization was 85.3 kJ/mol. The diffractogram of the product of the recrystallization process was the same as the diffractogram of the crystallized products.

4. Conclusions

In this work, LDME was crystallized from various solvents and recrystallized from the amorphous state. Thus, a presumably new polymorphic form of LDME could be easily prepared by solvent evaporation of EtOH, MeOH, water, precipitation from a solvent via dropping an antisolvent and solid-state recrystallization. The characteristic peaks on the XRP diffractogram of both assumable polymorphs were measured, according to the results, new peaks appeared in the case of all LDME products compared to LDME-I. The diffractogram of products was the same. According to the HPLC results, these changes were not due chemical composition of API. Besides the API was thermally analysed which showed a remarkable difference between the melting point of the different forms, the assignment of peaks was supported by additional HSM investigations. As an effect of heating to 145 °C, the LDME-EtOH was recrystallized to LDME-I explaining the exothermic peak appeared on the DSC curve above the melting point. The LDME-EtOH had the highest tendency to recrystallize, the LDME-MeOH had a lower tendency, in the case of LDME-water the recrystallization did not occur obviously. It was also concluded that the thermal stability of LDME was also decreased, it started decomposing after melting in both cases. Thus, as the melting point of the LDME product was lower, the thermal stability was also lower. The recrystallization kinetics of LDME was also measured by hot-humidity XRPD, based on these experiments, the activation energy of LDME recrystallization of amorphous LDME was 85.3 kJ/mol.

Acknowledgement

This work was supported by the ÚNKP-20-3-SZTE-316 New National Excellence Program of the Ministry for Innovation and Technology from the source of The National Research Development and Innovation Fund.

References

- Stocchi F, Marconi S. Factors Associated With Motor Fluctuations and Dyskinesia in Parkinson Disease: Potential Role of a New Melevodopa Plus Carbidopa Formulation (Sirio). *Clinical Neuropharmacology*. 2010 Jul;33(4):198-203.
- Pubchem open access chemistry database, compound summary of levodopa [cited 2021 May 11]. Available from: <https://pubchem.ncbi.nlm.nih.gov/compound/Levodopa>
- Fatma Haddad, Maryam Sawalha, Yahya Khawaja, Anas Najjar, Rafik Karaman. Dopamine and Levodopa Prodrugs for the Treatment of Parkinson's Disease. *Molecules*. 2017 Dec 25;23(1):40. <https://doi.org/10.3390/molecules23010040>
- Zangaglia R, Stocchi F, Sciarretta M, Antonini A, Mancini F, Guidi M, et al. Clinical Experiences With Levodopa Methylester (Melevodopa) in Patients With Parkinson Disease Experiencing Motor Fluctuations: An Open-Label Observational Study. *Clinical Neuropharmacology*. 2010 Mar;33(2):61-6. <https://doi.org/10.1097/WNF.0b013e3181c5e60c>
- Chun IK, Lee YH, Lee KE, Gwak HS. Design and Evaluation of Levodopa Methyl Ester Intranasal Delivery Systems. *Journal of Parkinson's Disease*. 2011;1(1):101-7. <https://doi.org/10.3233/JPD-2011-10011>
- Zhou YZ, Alany RG, Chuang V, Wen J. Studies of the Rate Constant of L-DOPA Oxidation and Decarboxylation by HPLC. *Chromatographia*. 2012 Jun;75(11-12):597-606. <https://doi.org/10.1007/s10337-012-2229-1>
- Isariebel Q-P, Carine J-L, Ulises-Javier J-H, Anne-Marie W, Henri D. Sonolysis of levodopa and paracetamol in aqueous solutions. *Ultrasonics Sonochemistry*. 2009 Jun;16(5):610-6. <https://doi.org/10.1016/j.ultsonch.2008.11.008>
- Fix JA, Alexander J, Cortese M, Engle K, Lepert P, Repta AJ. Short-Chain Alkyl Esters of L-Dopa as Prodrugs for Rectal Absorption. *Pharmaceutical Research*. 1989;06(6):501-5. <https://doi.org/10.1023/A:1015924724973>
- WuXi Labnetwork, information of [(2S)-3-(3,4-dihydroxyphenyl)-1-methoxy-1-oxopropan-2-yl] azanium;chloride [cited 2021 May 11]. Available from: <https://www.labnetwork.com/frontend-app/p/#!/moleculedetails/LN00194262>
- Hengartner D, Fernandez HH. The next chapter in symptomatic Parkinson disease treatments. *Parkinsonism & Related Disorders*. 2019 Feb;59:39-48. <https://doi.org/10.1016/j.parkreldis.2019.01.002>
- Leaflet of Sirio® [cited 2021 May 11]. Available from: <https://www.codifa.it/farmaci/s/sirio-melevodopa-carbidopa-antiparkinson-dopaminergici>
- Stocchi F, Fabbri L, Vecsei L, Krygowska-Wajs A, Monici Preti PA, Ruggieri SA. Clinical Efficacy of a Single Afternoon Dose of Effervescent Levodopa-Carbidopa Preparation (CHF 1512) in Fluctuating Parkinson Disease. *Clinical Neuropharmacology*. 2007 Jan;30(1):18-24.
- Chambridge Crystallographic Data Centre [cited 2021 May 11]. Available from: <https://www.ccdc.cam.ac.uk/>
- Florence AJ, Johnston A, Price SL, Nowell H, Kennedy AR, Shankland N. An Automated Parallel Crystallisation Search for Predicted Crystal Structures and Packing Motifs of Carbamazepine. *Journal of Pharmaceutical Sciences*. 2006 Sep;95(9):1918-30. <https://doi.org/10.1002/jps.20647>
- Pasquali I, Bettini R, Giordano F. Supercritical fluid technologies: An innovative approach for manipulating the solid-state of pharmaceuticals. *Advanced Drug Delivery Reviews*. 2008 Feb;60(3):399-410. <https://doi.org/10.1016/j.addr.2007.08.030>
- Terada K, Kurobe H, Ito M, Yoshihashi Y, Yonemochi E, Fujii K, et al. Polymorphic and pseudomorphic transformation behavior of acyclovir based on thermodynamics and crystallography. *J Therm Anal Calorim*. 2013 Sep;113(3):1261-7.
- Albers D, Galgoci M, King D, Miller D, Newman R, Peerey L, et al. Characterization of the Polymorphic Behavior of an Organic Compound Using a Dynamic Thermal and X-ray Powder Diffraction Technique. *Org Process Res Dev*. 2007 Sep;11(5):846-60.
- Friščić T, MacGillivray LR. Engineering cocrystal and polymorph architecture via pseudoseeding. *Chem Commun*. 2009;(7):773. <https://doi.org/10.1039/b820120j>
- Mazzobre MF, Soto G, Aguilera JM, Buera MP. Crystallization kinetics of lactose in systems co-lyophilized with trehalose. Analysis by differential scanning calorimetry. *Food Research International*. 2001 Jan;34(10):903-11.
- Fasano A, Bove F, Gabrielli M, Ragazzoni E, Fortuna S, Tortora A, et al. Liquid Melevodopa Versus Standard Levodopa in Patients With Parkinson Disease and Small Intestinal Bacterial Overgrowth. *Clinical Neuropharmacology*. 2014 Jul;37(4):91-5. <https://doi.org/10.1097/WNF.0000000000000034>